Viscoelastoplastic Model for Predicting Performance of Asphaltic Mixtures

JACOB UZAN, ARIEH SIDES, and MORDECHAI PERL

ABSTRACT

A mechanistic model for predicting performance of asphalt mixtures in terms of crack propagation rate, fatigue life assessment, and permanent deformation characteristics is presented. The model is based on stress evaluation by the finite element method and on a comprehensive viscoelastoplastic material law. A critical octahedral shear strain is assumed to be the failure criterion. A computer simulation of the resilient and residual deflections of uncracked beams as well as a fatigue crack growth simulation of an initially cracked beam are performed. These results are then compared with laboratory tests performed at various load levels with varying periods of loading and unloading. The agreement between the predicted and the measured performance of the sand-asphalt mixture in terms of residual and resilient deflection, crack length versus number of load applications, and rest period effect on fatigue life is found to be quite good. The simulation is then applied to predict rutting parameters, fatigue life curves, and crack propagation rate versus stress intensity factor for the sand-asphalt mixture.

The rational structural design of flexible pavements is well established and has already reached the stage of calibration and verification. In the calibration phase it has been found that some aspects related to material characterization, such as the effects of the crack growth process and of the rest period on the fatigue life of bituminous mixtures, have been ignored. These effects are presently being accounted for during the design procedure by the use of correction factors that vary from 1 (where no correction is needed) to 700 (1-4). It appears that these correction factors are dependent on material and load as well as on environmental conditions and should therefore be determined specifically at each particular site.

Extensive laboratory and field studies of bituminous mixture fatigue performance clearly indicate that

- An increase of the rest period ratio prolongs fatigue life by a factor of up to 25 (5-8);
- The main part of fatigue life consists of the crack growth stage, which is considerably longer than the crack initiation phase (2-3);
- The crack grows according to Paris' law (9-12); and
- The testing program required for a complete fatigue performance characterization is prohibitively large and impractical.

From these results it is evident that a rational and more accurate prediction model for fatigue life of bituminous mixtures is required.

It is the purpose of this paper to present an improved mechanistic model for fatigue crack growth prediction incorporating the rest period effect. The model is based on a comprehensive material law accounting for the elastic, plastic, viscoelastic, and viscoplastic strain components (13-14). Because there are a limited number of different bituminous mixtures, this model can also be used statewide to optimize mix design.

Following the material characterization testing program and the results, the proposed mechanistic model for fatigue crack growth prediction is presented. Then numerical results and experimental verification for fatigue crack growth in sand-asphalt are given including an analysis of the rest period ratio effect.

MATERIAL CHARACTERIZATION

In the present study it is crucial to decompose the material's response to loading into time-dependent and time-independent strain components as well as into recoverable and irrecoverable ones. The repetitive creep test is found to be most appropriate to comply with this required resolution. Uniaxial compressive and tensile repetitive creep tests are therefore to be conducted at 25°C, using a sand-asphalt mixture. Details of the mixture properties, the experimental procedure, and the results of the compression tests are presented elsewhere (13). Recently these experiments were supplemented by a series of tension tests to account for the different responses of the mixture to tensile and compressive loading. These results are published elsewhere (14).

The total strain (ϵ_t) is thus resolved into its four components (Figure 1):

$$\epsilon_t = \epsilon_e + \epsilon_p + \epsilon_{ve} + \epsilon_{vp} \quad (1)$$

where

- ϵ_e = elastic strain--recoverable and time independent,
- ϵ_p = plastic strain--irrecoverable and time independent,
- ϵ_{ve} = viscoelastic strain--recoverable and time dependent, and
- ϵ_{vp} = viscoplastic strain--irrecoverable and time dependent.

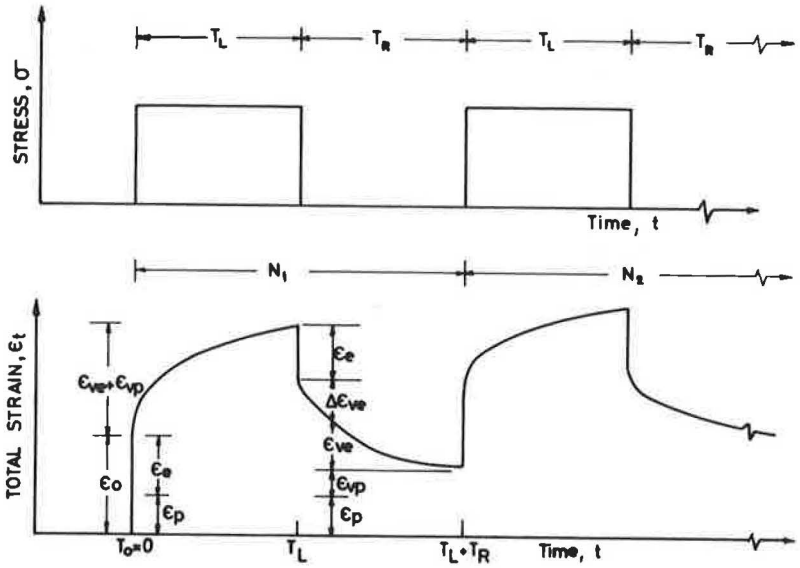

FIGURE 1 Schematic representation of the various strain components.

Each strain component is expressed as a function of the stress level, loading time, and number of repetitions as follows:

$$\epsilon_e = \sigma/E \tag{2}$$

$$\epsilon_p = (\sigma/H)\, N^a \tag{3}$$

$$\epsilon_{ve} = (a_1 \sigma + a_2 \sigma^2) t^{\alpha} \tag{4}$$

$$\epsilon_{vp} = (b_1 \sigma + b_2 \sigma^2) T_L{}^{\beta} N^b \tag{5}$$

where

σ = applied stress (MPa);
E = elastic modulus (MPa);
H = plastic modulus (MPa);
N = number of load repetitions;
t = time elapsing from the beginning of the test (sec);
T_L = loading time during each cycle (sec); and
$a, a_1, a_2, \alpha, b, b_1, b_2, \beta$ = material constants.

The experimentally evaluated values for the various parameters in Equations 2-5 are given in Table 1.

In the uniaxial creep repetitive tensile tests it was found that the total strain at failure is in the range of 0.8 to 2.2 percent for a stress level of 0.05 to 0.1 MPa. Similar results, 0.4 to 0.8 and 1.0 to 2.5 percent, are reported by Monismith et al. (15) and Tons and Krokosky (16) for constant strain rate and creep tests of asphalt concrete at 25°C (77°F). For the case of high asphalt content and low strain rate corresponding to the present testing conditions, it appears that the uniaxial tensile strain of failure is 0.8 to 2.5 percent. Because it is intended to apply these values to multiaxial loading, the failure strain is replaced by the critical octahedral shear strain corresponding values of which are 1.1 to 3.3 percent (for a Poisson's ratio of 0.4). To overcome the range of critical strain experimentally measured, a parametric study of sensitivity will be conducted.

TABLE 1 Material Constants of the Strain Components

	Unit	Compression	Tension
E	MPa	613	590
H	MPa	278.5	∞
a		0.35	
a_1	MPa^{-1}	8.9×10^{-4}	9.4×10^{-4}
a_2	MPa^{-2}	-5.0×10^{-4}	0
α	0	0.29	0.58
b		0.19	0.62
b_1	MPa^{-1}	1.9×10^{-3}	5.9×10^{-4}
b_2	MPa^{-2}	-8.4×10^{-4}	0
β		0.22	0.27

FATIGUE CREEP CRACK GROWTH SIMULATION

A mechanistic model is developed for the simulation of fatigue creep crack growth. Further on the simulation is applied to the three-point bend specimen (i.e., a simple supported beam loaded by a time-varying uniformly distributed load applied at its midspan). By superposing loading and unloading periods of different durations, the repetitive character of the cyclic loading is reproduced and various rest period ratios are possible.

To make the simulation feasible the model was simplified on the basis of the following assumptions:

1. The stress distribution in the specimen is evaluated for a homogeneous, isotropic, linear elastic material by the finite element method.
2. Equivalent loading and unloading moduli of deformation are evaluated using the constitutive law determined for the uniaxial compressive and tensile repetitive creep test and on a strain energy consideration.
3. Strains are evaluated using stresses and the equivalent loading or unloading moduli of deformation.
4. The crack is assumed to grow upward when the octahedral shear strain in the vicinity of the crack tip reaches its critical value.
5. The crack is extended by applying the unzipping procedure, with an increment that equals one mesh size of the finite element grid.

6. As the crack grows, the stress field ahead of the crack tip changes.

The equivalent number of cycles corresponding to the new state of stress field is evaluated using a time-hardening scheme (17).

It should be noted that assumptions 1 to 3 do not strictly comply with the compatibility conditions of continuum and thus neglect the stress redistribution occurring in the beam. Experimental verification of the adequacy of these assumptions and approximations will be presented in the next section. The failure criterion is discussed separately.

The fatigue creep crack growth simulation is incrementally performed. Each step is associated with a specific crack size. Initially the beam is assumed to have a small crack on its centerline, emanating from its lower side, which is in tension. Furthermore, the beam is stress and strain free. During subsequent steps, as the crack extends, the accumulated strains and the number of cycles of each step serve as initial conditions for the next one.

The simulation pursues the following algorithm for the first step: for a given initial crack length the stress distribution in the three-point bend specimen is determined via the NONSAP finite element code (18). (For details on the geometry of the specimen and the finite element breakdown see Figure 2). The stress along the centerline of the beam ahead of the crack tip is evaluated at the nodal points and is then averaged for each two adjacent elements to provide a unique distribution of stress on the crack line. Equivalent loading and unloading moduli of deformation representing the beam are computed using the following equation, which is based on equal strain energy considerations:

$$1/\bar{E} = \left\{ \sum_{i=1}^{n} (1/E_i) \left[\sigma_{xx}^{(i)2} + \sigma_{yy}^{(i)2} - 2\mu\sigma_{xx}^{(i)} \sigma_{yy}^{(i)} \right] \right\} \div \left\{ \sum_{i=1}^{n} \left[\sigma_{xx}^{(i)2} + \sigma_{yy}^{(i)2} - 2\mu\sigma_{xx}^{(i)} \sigma_{yy}^{(i)} \right] \right\} \quad (6)$$

where

$\bar{E}$ = equivalent loading or unloading modulus of deformation,
$\sigma_{xx}^{(i)}$, $\sigma_{yy}^{(i)}$ = stress components (i denotes nodal point number), and
E_i = modulus of deformation at ith nodal point evaluated by Equations 1-5.

Using the equivalent modulus and stress field the incremental octahedral shear strain caused during the nth loading cycle is evaluated at all nodal points and is added to the previously accumulated octahedral shear strain. The total octahedral shear strain near the crack tip is compared with its assumed critical value. If the critical value is not reached, unloading is performed and the incremental resilient octahedral shear strain is determined and subtracted from the previously accumulated strain. Cyclic loading and unloading are repeated for the same crack length and stress distribution until the total octahedral shear strain ahead of the tip reaches its critical value. When this occurs the crack is extended by one mesh size (one element length) and stresses are reevaluated for the new geometric configuration. The accumulated number of load repetitions at all nodal points ahead of the crack tip is replaced by an equivalent initial number of repetitions that corresponds to the accumulated octahedral shear strain, the new state of stress, and the new crack length. This updating procedure is based on a time-hardening scheme and is independently performed for the plastic and viscoplastic strain components. The crack extension procedure described herein is then repeated until unstable crack length occurs.

For each crack length, the mode I stress intensity factor (K_I) is evaluated from the finite element solution via the vertical displacement of the quarter point of the singular isoparametric element (19,20, see Figure 2). The stress intensity factor is used in the analysis.

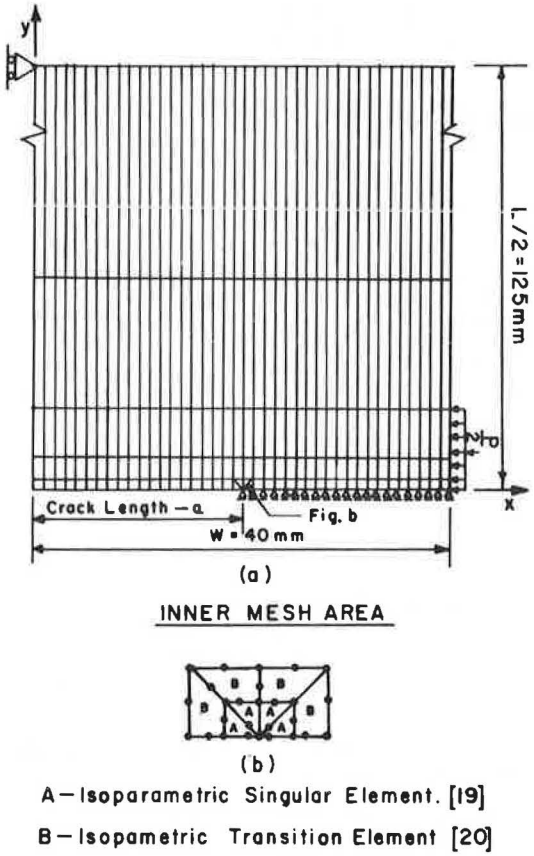

FIGURE 2 Geometry of the specimen and finite element breakdown.

Crack Growth Criterion

In the unzipping procedure, the crack is advanced by one mesh size increments. It is obvious that the results of the analysis are dependent on the mesh size and the distance from the crack tip at which the strain is calculated.

Sensitivity analyses show that when the strain is calculated at one-eighth of the mesh size ahead of the crack tip, the numerical results of load repetition are almost independent of the mesh size. Therefore, as a numerical stability consideration, the point located one-eighth mesh size from the crack tip is adopted in the simulation process.

The crack is extended as the mean octahedral shear strain within the element ahead of the crack tip reaches its critical value. Because the analysis is performed employing the one-eighth point, the fracture can be expressed as

$$\gamma_{oct}^{1/8} \geq 2^{1/2} \cdot \gamma_{oct}^{cr} \quad (7)$$

where

$\gamma_{oct}^{1/8}$ = octahedral shear strain at the one-eighth point and
γ_{oct}^{cr} = octahedral shear strain at failure.

EXPERIMENTAL VERIFICATION

A testing program was designed to provide verification of the various assumptions and approximations made throughout the simulation process. It includes repetitive creep tests in bending of uncracked beams and fatigue tests on initially cracked ones. The

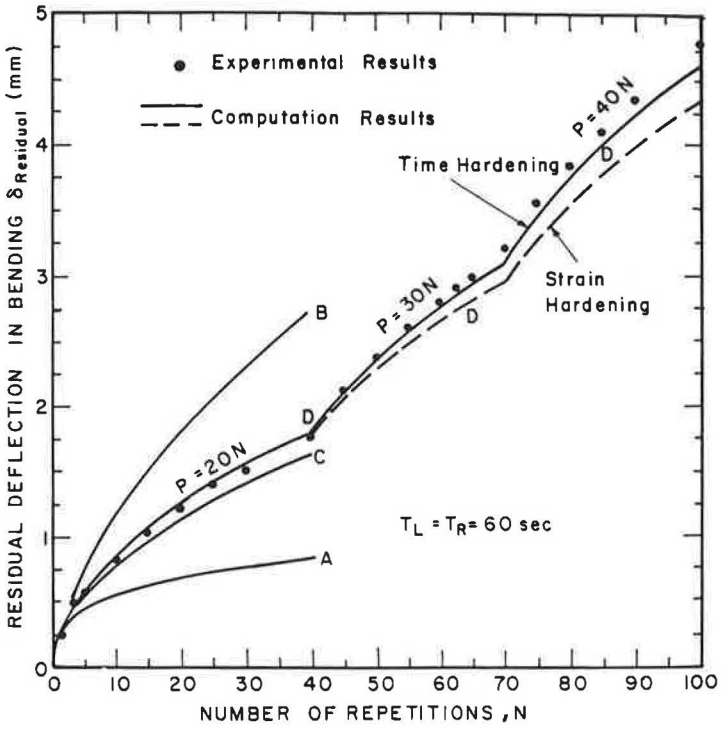

FIGURE 3 Experimental and computed residual deflection at varying cyclic loading ($T_L = T_R = 60$ sec).

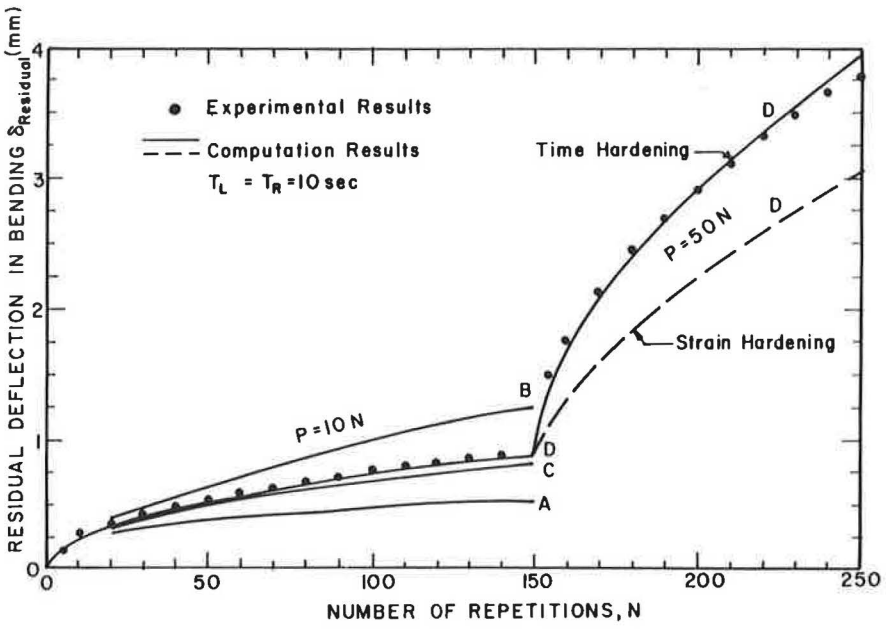

FIGURE 4 Experimental and computed residual deflection at varying cyclic loading ($T_L = T_R = 10$ sec).

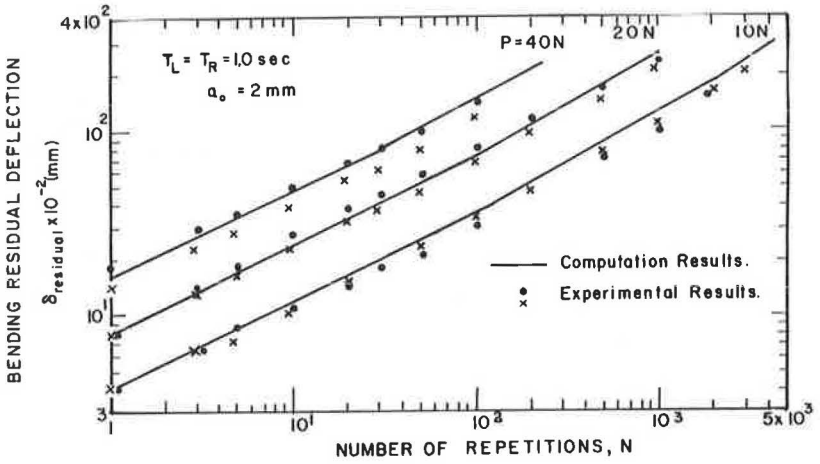

FIGURE 5 Experimental and computed residual deflection for initially cracked beam ($T_L = T_R = 1.0$ sec).

residual and the resilient deflections as well as crack lengths for various load levels, loading and unloading durations (T_L and T_R, respectively), and initial crack lengths were recorded as a function of load cycle number. Some results are presented hereafter.

Residual Deflection of Uncracked Beams

The residual deflection of uncracked beams subjected to a varying cyclic loading is shown in Figures 3 and 4. The results obtained when applying the first load level serve to develop a procedure for determining the equivalent loading and unloading moduli.

The residual deflection at the beam midspan after N loading cycles $[\delta^{(N)}_{residual}]$ is computed using the following equation (21):

$$\delta^{(N)}_{residual} = \sum_{i=1}^{N} \Delta\delta_i = \sum_{i=1}^{N} \delta_o \left[(E_o/\bar{E}^{(N)}_{\ell o}) - (E_o/\bar{E}^{(N)}_{un\ell o})\right] \quad (8)$$

where

δ_o = deflection corresponding to the finite element analysis;
E_o = modulus of deformation corresponding to finite element solution; and
$\bar{E}^{(N)}_{\ell o}$, $\bar{E}^{(N)}_{un\ell o}$ = equivalent loading and unloading moduli of deformation, respectively.

The loading and unloading moduli necessary for the numerical evaluation of the residual deflection are calculated by four different methods: (a) compressive material constants (Curve A); (b) tensile material constants (Curve B); (c) bilinear material equation (22, Curve C):

$$\bar{E} = (4 \cdot E_{com} \cdot E_{ten})/(E_{com}^{1/2} + E_{ten}^{1/2})^2 \quad (9)$$

where E_{com} and E_{ten} are the compression and tension moduli of deformation, respectively, for loading or unloading; and (d) from strain energy considerations (Curve D) as expressed in Equation 6. The method of equal strain energy is found to be adequate and is therefore adopted in the simulation process.

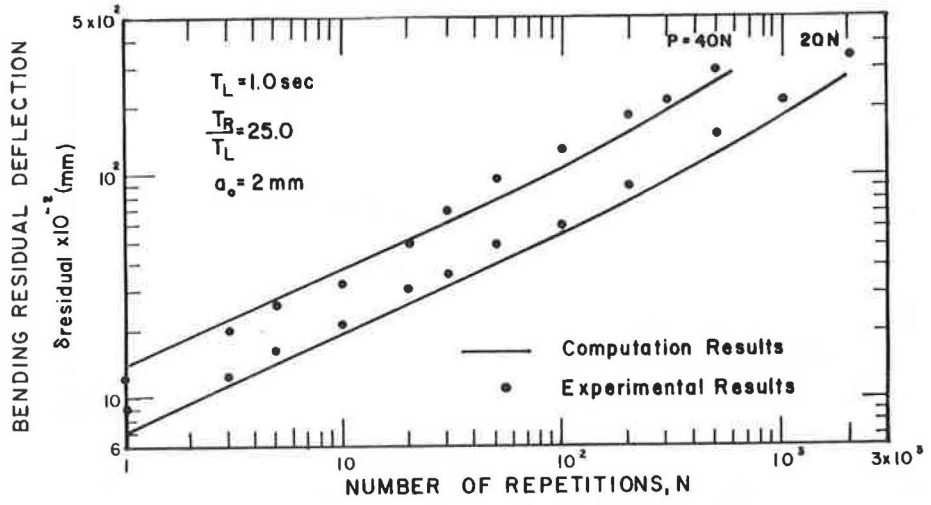

FIGURE 6 Experimental and computed residual deflection for initially cracked beam ($T_R/T_L = 25.0$).

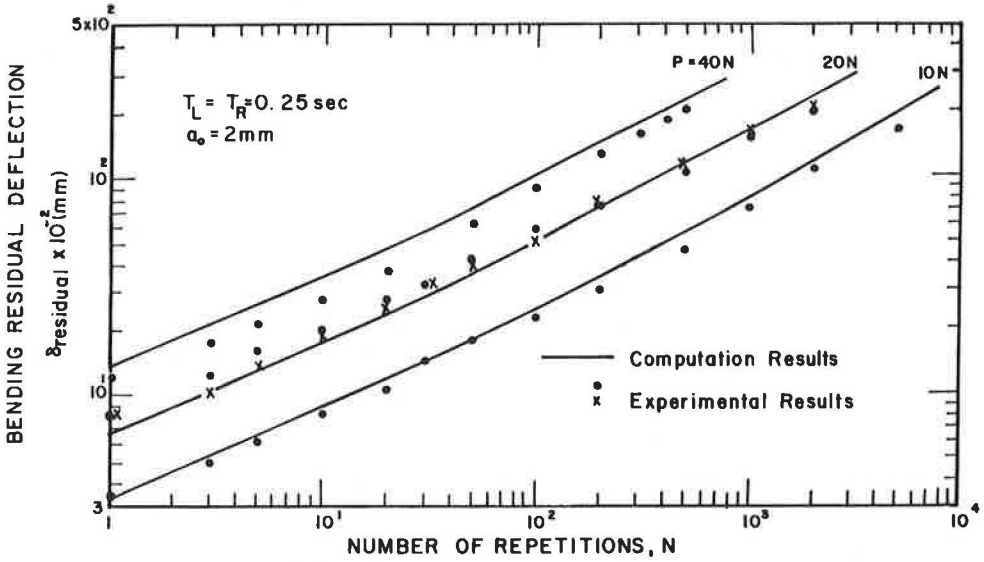

FIGURE 7 Experimental and computed residual deflection for initially cracked beam ($T_L = T_R = 0.25$ sec).

The subsequent load levels are used to determine which superposition method should be used in the case of increasing load. In Figures 3 and 4 the residual deflection evaluated by both time- and strain-hardening procedures is presented with the experimental results. It can be seen that time hardening is more adequate and fits the experimental results quite well. It should be mentioned that similar results were reported by Monismith (17).

Residual Deflection of Cracked Beams

Fatigue test results for cracked beams in bending are shown in Figures 5-7. These results correspond to an initially cracked beam subjected to different load levels with various loading and unloading periods. The residual deflections were computed using Equations 6 and 8. It can be seen that the simulation prediction is good and is thus applicable to the loading-to-unloading ratio effect on the pavement.

Crack Length Versus Number of Cycles

Crack length versus the number of load repetitions for various initial crack lengths, load levels, and T_R and T_L are shown in Figures 8-13. For each particular case three predicted curves are shown corre-

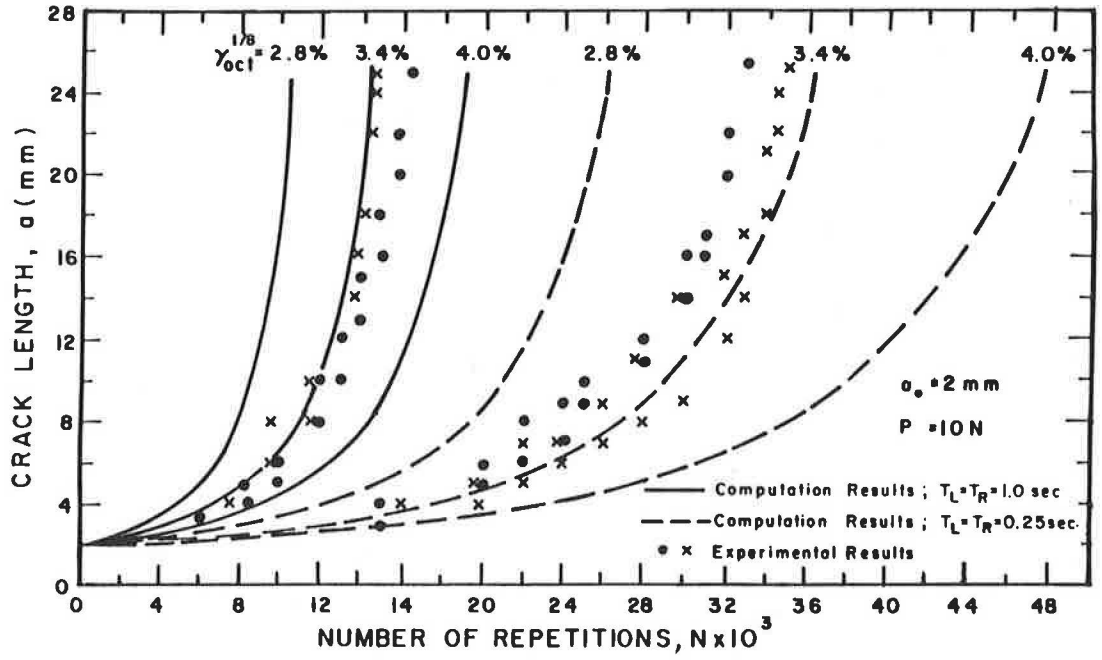

FIGURE 8 Experimental and predicted a–N curve for P = 10 N.

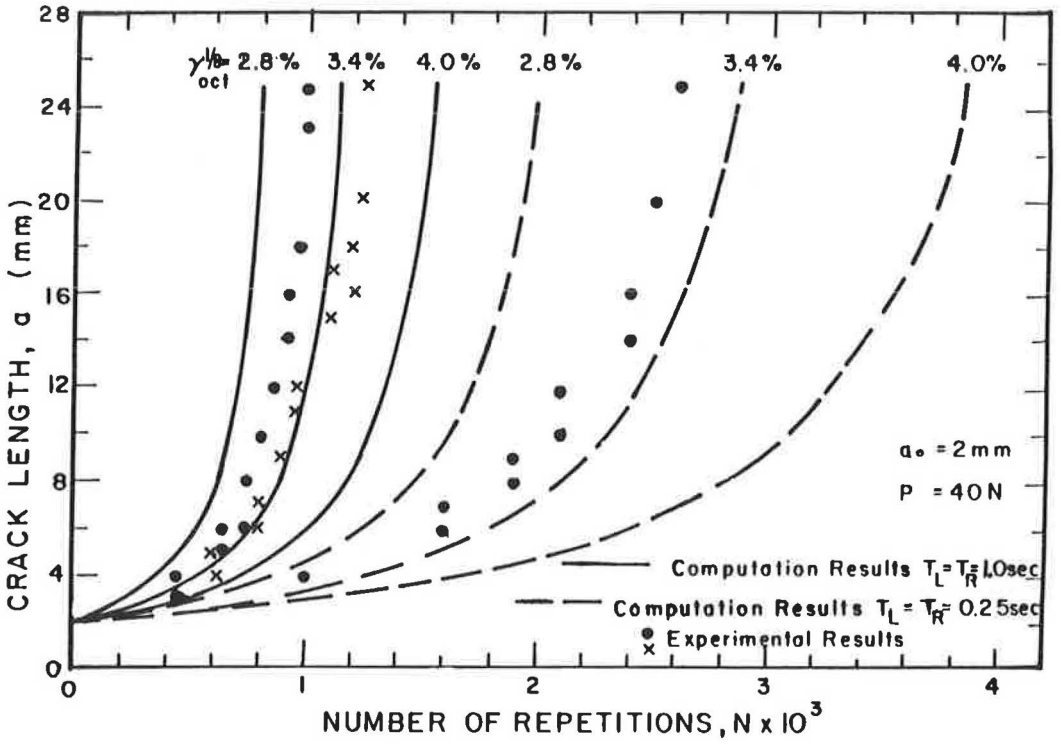

FIGURE 9 Experimental and predicted a–N curve for P = 40 N.

sponding to $\gamma_{oct}^{1/8}$ = 2.8, 3.4, and 4.0 percent critical octahedral shear strain. It appears that the predicted results are in better agreement with the experimental data for a critical octahedral shear strain of 3.4 percent. It is worth mentioning that this value corresponds to the upper limit of the uniaxial tension test results reported previously.

Table 2 gives the predicted and experimental fatigue life (N_T and N_p, respectively) and their ratio. The ratio N_p/N_T is found to be in the range of 0.81 to 1.20 for all cases.

These results, although not yet fully verified, support the validity of this simulation procedure, which therefore might be used for permanent deforma-

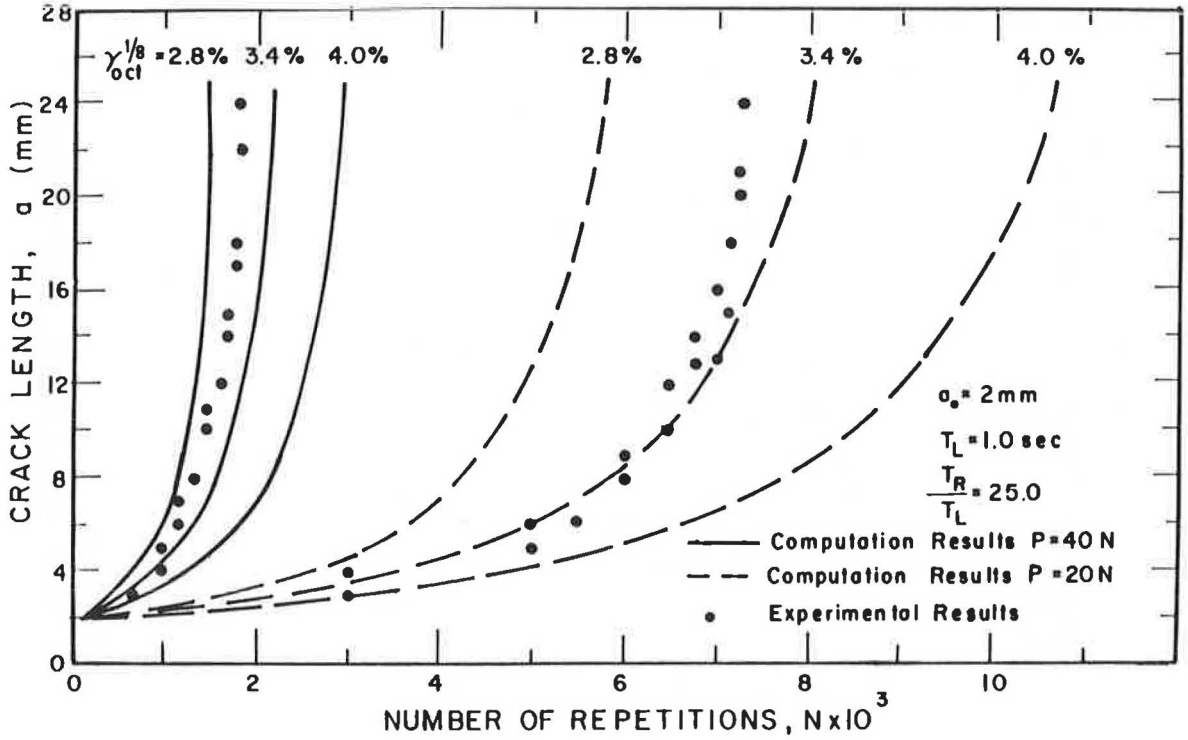

FIGURE 10 Experimental and predicted a–N curve for T_R/T_L = 25.0.

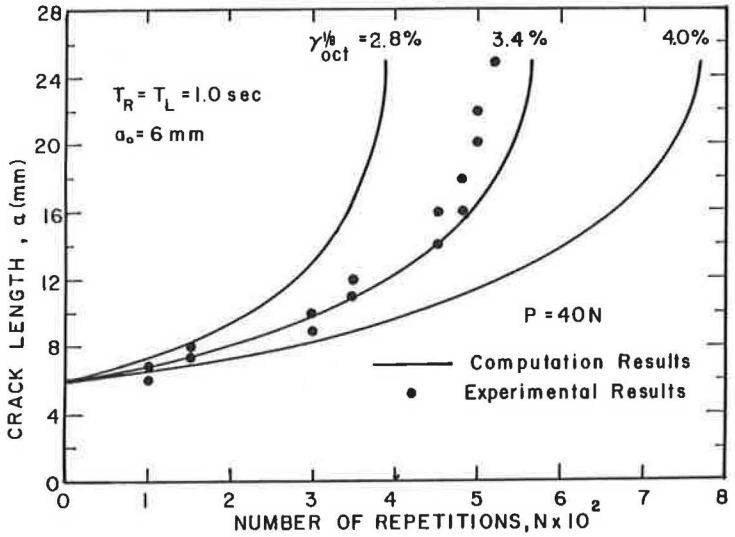

FIGURE 11 Experimental and predicted a–N curve for a_o = 6 mm.

tion characterization and for fatigue life assessment of the sand-asphalt mixture.

PERMANENT DEFORMATION OF SAND-ASPHALT MIXTURES

In permanent deformation analyses of pavements the relevant parameters commonly used are α and μ that describe the residual strain versus the number of load repetitions (23–26). The test results (see Figure 3) as well as the ones predicted (by Equations 1-6) given in Table 3 indicate that the value of these parameters depends on the loading mode: compression, tension, or bending. The values for the bending mode case are as expected; they are situated between those obtained in compression and those obtained in tension. This conclusion points out that the compressive creep test may be inadequate for describing the permanent deformation characteristics of asphaltic materials.

FATIGUE LIFE PREDICTION

In the previous section it was shown that the model predicts fatigue creep crack growth quite well (Figures 8-13 and Table 2). In this section the fatigue life prediction will be expressed in engineering terms: bending tensile strain versus number of load repetitions to failure, the effect of the rest period, and Paris' law.

ε-N Curve

Two predicted ε-N curves simulated for two different loading periods together with experimental results from Monismith et al. (27) and Pell and Cooper (28) are shown in Figure 14. The predicted values are in good agreement with those of Monismith et al. for similar mixture stiffness.

Pell's and Cooper's results are well below the predicted ones. However, Pell's and Cooper's results were found by Witczak (29) to be on the conservative side compared to most results reported in the literature. Thus it may be concluded that the prediction is quite good.

Effect of Rest Period

The beneficial effect of the rest period between consecutive loading phases is well established

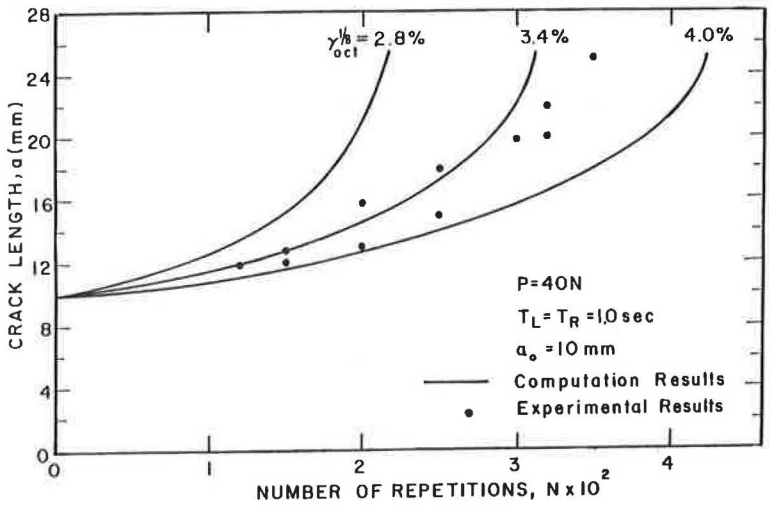

FIGURE 12 Experimental and predicted a–N curve for a_o = 10 mm.

TABLE 2 Predicted and Experimental Crack Growth Repetitions

Loading Period T_L (sec)	T_R/T_L	Initial Crack Length a_o (mm)	Load Level P (N)	Predicted Fatigue Life N_p	Experimental Fatigue Life N_T	N_p/N_T
			10	14,654	14,522-16,493	0.89-1.01
1.0	1.0	2.0	20	4,240	4,482-5,170	0.82-0.95
			40	1,154	1,007-1,260	0.92-1.15
1.0	5.0	2.0	20	5,894	5,550	1.07
			40	1,590	1,329	1.20
			20	8,067	7,400	1.09
1.0	25.0	2.0	40	2,168	1,847	1.17
			10	36,397	33,080-35,211	1.03-1.10
0.25	1.0	2.0	20	10,533	9,879-11,166	0.94-1.07
			40	2,863	2,601	1.10
			20	14,544	14,629	0.99
0.25	8.0	2.0	40	3,945	4,895	0.81
		6.0		574	511	1.12
1.0	1.0	10.0	40	315	351	0.90
		14.0		166	138	1.20

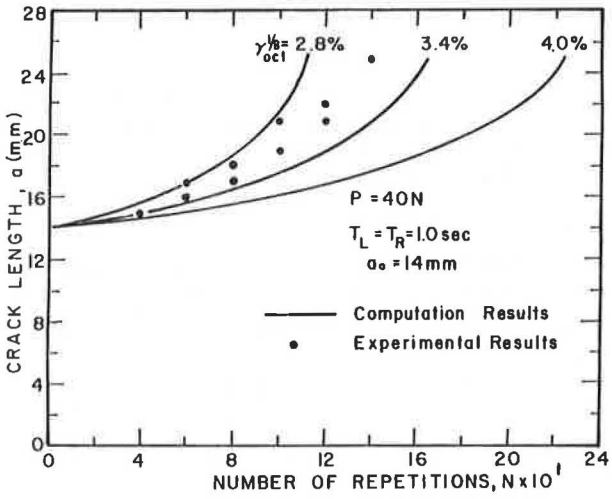

FIGURE 13 Experimental and predicted a-N curve for a_o = 14 mm.

(5-8). From Figures 9 and 10 and Table 2 it can be found that for a rest period ratio of 25 (T_R/T_L = 25) and a load of 40 N, fatigue life is increased by a factor of 1.47 to 1.83 with respect to the experimental results and by a factor of 1.9 with respect to the predicted one. Furthermore, the results in Table 2 indicate that the effect of the rest period depends on the loading duration.

TABLE 3 Test and Computed Results of the α and μ Parameters

	Compression	Tension	Bending
Test Results, $T_L = T_R$ = 60 sec			
α	0.67	0.38	0.49
μ	0.72	0.43	0.60
Computed Results, $T_L = T_R$ = 0.1 sec			
α	0.67	0.38	0.59
μ	0.63	0.15	0.45

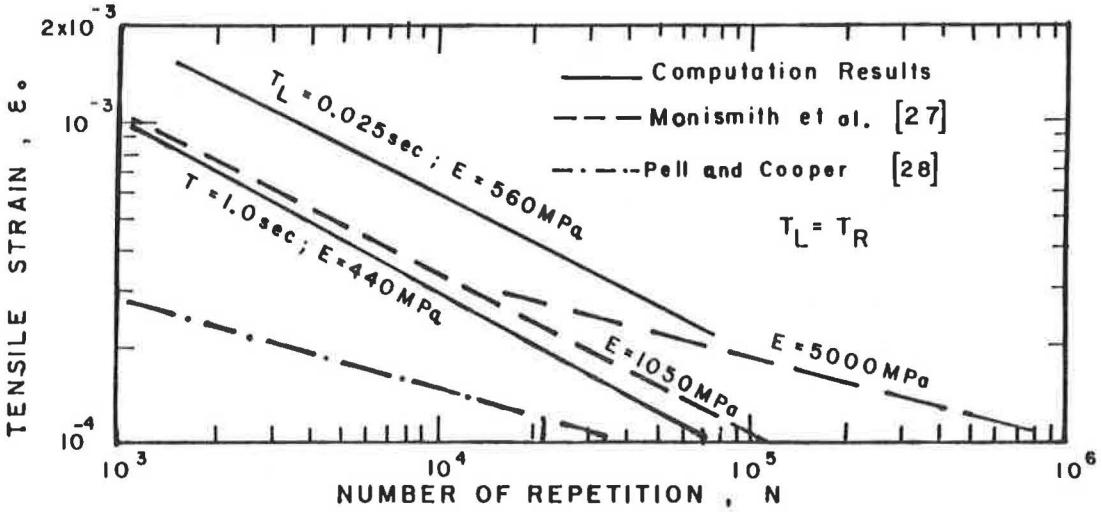

FIGURE 14 Predicted tensile strain versus number of load repetitions.

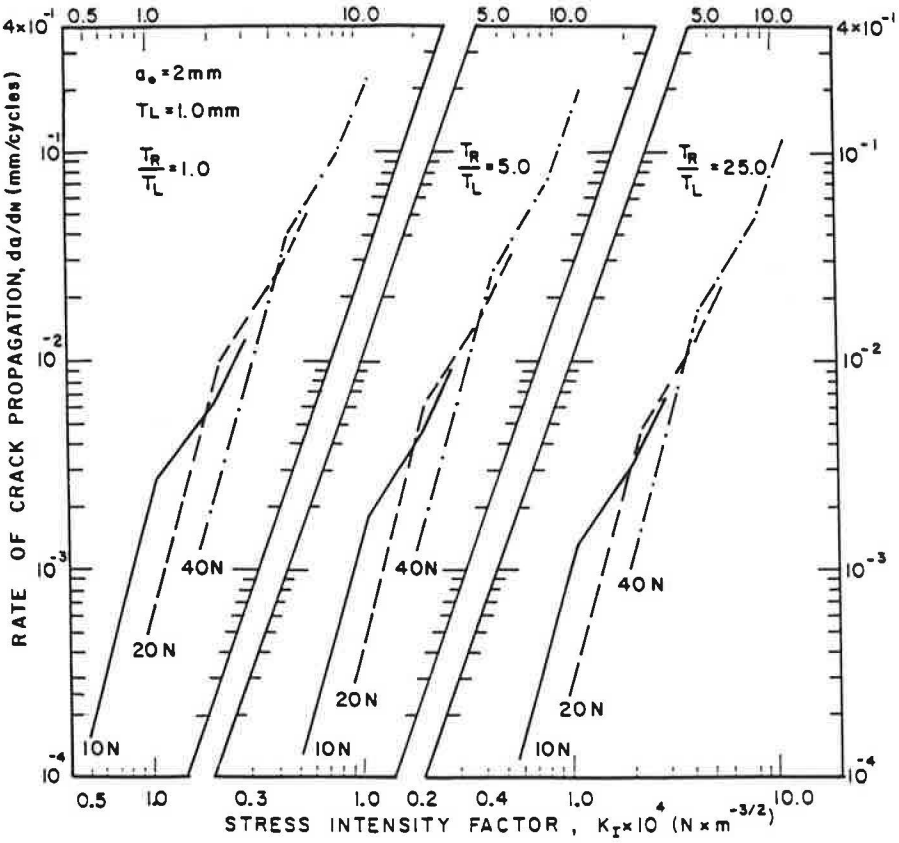

FIGURE 15 Predicted da/dN versus K_I for various T_R/T_L.

Paris' Law

Fatigue life prediction as well as crack repetition in asphaltic material have recently been dealt with using the fracture mechanics theory approach and in particular Paris' law (9-12), that is,

$$da/dN = A K_I^n \quad (10)$$

where

a = crack length,
N = number of load applications,
K_I = mode I stress intensity factor, and
A,n = material constants.

The stress intensity factor as previously mentioned is evaluated from the finite element analysis. The crack propagation rate (da/dN) can be calculated both from the experimental results and from the simulated a-N curve. Predicted relations between the crack propagation rate and the stress intensity factor are shown in Figures 15 and 16. From these figures it can be seen that

1. The relation between da/dN and K_I is load dependent to a certain extent. A similar dependence is noted in the test results of Majidzadeh et al. (9,12).
2. The curve consists of three distinguishable segments for a small initial crack case, which tend to become one line as initial crack length increases.
3. The crack growth rate depends on the initial crack length (see Figure 16).

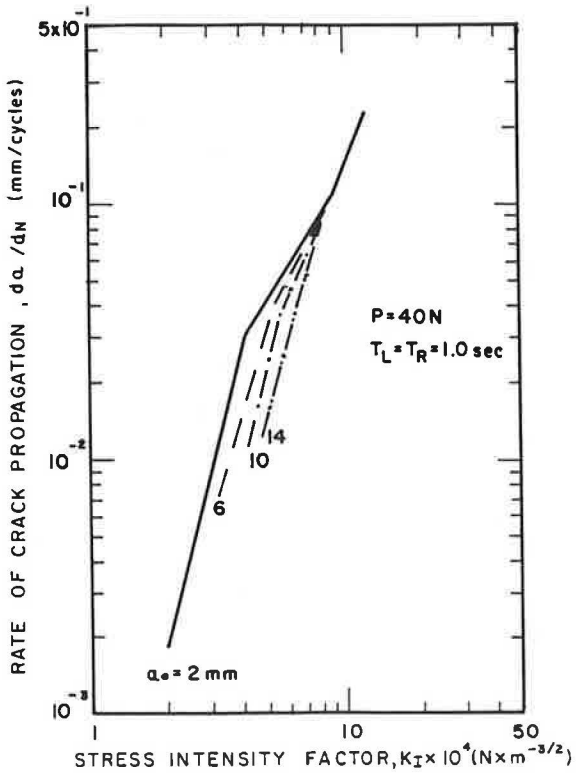

FIGURE 16 Predicted da/dN versus K_I for various initial crack lengths.

An effort to include the loading level, the loading and unloading durations, and the initial crack length in one Paris-like law is presently being made.

SUMMARY

A mechanistic model for predicting performance of sand-asphalt mixtures is presented and verified by laboratory tests. The model is found to give good results for a broad range of variables: load levels, loading and unloading durations, and initial crack lengths. It is shown that the model is adequate for predicting permanent deformation characteristics and the fatigue life of the sand-asphalt mixture used in the present research. It can therefore be applied confidently to the parametric study of the performance of asphalt material with a limited test program.

ACKNOWLEDGMENT

This research was supported by the Technion Vice-President for Research Funds through the L. Edelstein Research Fund.

REFERENCES

1. S.F. Brown and P.S. Pell. A Fundamental Structural Design Procedure for Flexible Pavements. Proc., 3rd International Conference on the Structural Design of Asphalt Pavements, London, England, Vol. 1, Sept. 1972, pp. 326-342.
2. W. Van Dijk. Practical Fatigue Characterization of Bituminous Mixes. Proc., Association of Asphalt Paving Technologists, Vol. 44, 1975, pp. 38-74.
3. S.F. Brown, J.M. Brunton, and P.S. Pell. The Development and Implementation of Analytical Pavement Design for British Conditions. Proc., 5th International Conference on the Structural Design of Asphalt Pavements, Delft, The Netherlands, Vol. 1, Aug. 1982, pp. 3-16.
4. N.W. Lister, W.D. Powell, and R.T.N. Goddard. A Design for Pavement to Carry Very Heavy Traffic. Proc., 5th International Conference on the Structural Design of Asphalt Pavements, Delft, The Netherlands, Vol. 1, Aug. 1982, pp. 84-91.
5. K.D. Raithby and A.D. Sterling. Some Effects of Loading History on the Fatigue Performance of Rolled Asphalts. TRRL Report LR 496. Transport and Road Research Laboratory, Department of the Environment, Crowthorne, Berkshire, England, 1972.
6. L. Francken. Fatigue Performance of a Bituminous Road Mix Under Realistic Test Conditions. In Transportation Research Record 712, TRB, National Research Council, Washington, D.C., 1979, pp. 30-37.
7. W. Van Dijk and W. Vinner. The Energy Approach to Fatigue for Pavement Design. Proc., Association of Asphalt Paving Technologists, Vol. 46, 1977, pp. 1-40.
8. F.D. Bonnaure, A.H.J.J. Huibers, and A. Boonders. A Laboratory Investigation of the Influence of Rest Periods on the Fatigue Characteristics of Bituminous Mixes. Proc., Association of Asphalt Paving Technologists, Vol. 52, 1982, pp. 104-128.
9. K. Majidzadeh, D.V. Ramsamooj, and A.T. Chan. Analysis of Fatigue and Fracture of Bituminous Paving Mixtures. Project RF-2845, Phase I. Ohio State University Research Foundation, Columbus, 1970.
10. D.V. Ramsamooj. Fatique Cracking of Asphalt Pavements. In Transportation Research Record 756, TRB, National Research Council, Washington, D.C., 1981, pp. 43-48.
11. K. Majidzadeh, E.M. Kauffman, and C.L. Saraf. Analysis of Fatigue of Paving Mixtures from the Fracture Mechanics Viewpoint. STP 508. ASTM, 1972, pp. 67-83.
12. K. Majidzadeh, C. Buranarom, and M. Karakomzian. Application of Fracture Mechanics for Improved Design of Bituminous Concrete. Report FHWA-RD-76-92. FHWA, U.S. Department of Transportation, Vol. 2, 1976.
13. M. Perl, J. Uzan, and A. Sides. Visco-Elasto-Plastic Constitutive Law for a Bituminous Mixture Under Repeated Loading. In Transportation Research Record 911, TRB, National Research Council, Washington, D.C., 1983, pp. 20-27.
14. A. Sides, J. Uzan, and M. Perl. A Comprehensive Visco-Elasto-Plastic Characterization of Sand-Asphalt under Compression and Tension Cyclic Loading. ASTM, Journal of Testing and Evaluation, Vol. 13, No. 1, 1985, pp. 49-59.
15. C.L. Monismith, G.A. Secor, and K.E. Secor. Temperature Induced Stresses and Deformation in Asphalt Concrete. Proc., Association of Asphalt Paving Technologists, Vol. 34, 1965, pp. 248-285.
16. E. Tons and E.M. Krokosky. Tensile Properties of Dense Graded Bituminous Concrete. Proc., Association of Asphalt Paving Technologists, Vol. 32, 1963, pp. 497-529.
17. C.L. Monismith. Rutting Prediction in Asphalt Concrete. In Transportation Research Record 616, TRB, National Research Council, Washington, D.C., 1976, pp. 2-8.
18. K.J. Bathe, E.L. Wilson, and R.H. Iding. NONSAP--A Structural Analysis Program for Static and Dynamic Response of Nonlinear Systems. Report 74-3. Structural Engineering Laboratory, University of California, Berkeley, Feb. 1974.
19. R.S. Barsoum. On the Use of Isoparametric Finite Element in Linear Fracture Mechanics. International Journal for Numerical Methods in Engineering, Vol. 10, 1976, pp. 15-37.
20. P.P. Lynn and A.R. Ingraffea. Transition Elements to be Used with Quadratic Point Crack Tip Elements. International Journal of Numerical Methods in Engineering, Vol. 12, 1978, pp. 1031-1038.
21. J. Uzan. Permanent Deformation in Pavement Design and Evaluation. International Symposium on Bearing Capacity of Roads and Airfields, Trondheim, Norway, Vol. 2, 1982, pp. 658-669.
22. S. Timoshenko and J.N. Goodier. Theory of Elasticity. 2nd ed. McGraw-Hill Book Co., New York, 1951, 506 pp.
23. R.L. Lytton, D. Saylak, and D.E. Pickett. Prediction of Sulphur-Asphalt Pavement Performance with VESIS IIM. Proc., 4th International Conference on the Structural Design of Asphalt Pavements, University of Michigan, Ann Arbor, Vol. 1, Aug. 1977, pp. 855-861.
24. C.L. Monismith, K. Inkabi, C.F. Freeme, and D.B. McLean. A Subsystem to Predict Rutting in Asphalt Concrete Pavement Structures. 4th International Conference on the Structural Design of Asphalt Pavements, University of Michigan, Ann Arbor, Vol. 1, Aug. 1977, pp. 529-539.
25. J.B. Rauhut, R.C.G. Haas, and T.W. Kennedy. Comparison of VESYS IIM Predictions to Brampton/AASHO Performance Measurements. Proc., 4th International Conference on the Structural Design of Asphalt Pavements, University of Michigan, Ann Arbor, Vol. 1, Aug. 1977, pp. 131-138.

26. J. Verstaten, J.E. Romain, and V. Veverka. The Belgian Road Research Centre's Overall Approach to Asphalt Pavement Structural Design. Proc., 4th International Conference on the Structural Design of Asphalt Pavements, University of Michigan, Ann Arbor, Vol. 1, Aug. 1977, pp. 298-324.
27. C.L. Monismith, K.E. Secor, and E.W. Blackmer. Asphalt Mixture Behaviour in Repeated Flexure. Proc., Association of Asphalt Paving Technologists, Vol. 30, 1961, pp. 188-222.
28. P.S. Pell and K.E. Cooper. The Effect of Testing and Mix Variables on the Fatigue Performance of Bituminous Materials. Proc., Association of Asphalt Paving Technologists, Vol. 44, 1975, pp. 1-37.
29. M.W. Witczak. Pavement Performance Models Repeated Load Fracture of Pavement Systems. Report 5-76-15, FAA DOT-FA 73WAI-377. FHWA, U.S. Department of Transportation, Vol. 1, 1977, 193 pp.

Publication of this paper sponsored by Committee on Flexible Pavements.

Load Rating of Light Pavement Structures

KOON MENG CHUA and ROBERT L. LYTTON

ABSTRACT

A new approach to determining the damage that overweight vehicles can do to light pavement structures is described. This procedure uses deflections measured with either the Dynaflect or the falling weight deflectometer to determine the number of passes of a specific load that will cause a critical level of rut depth in a light pavement structure. This method was based on field observations and ILLI-PAVE, a finite element pavement analysis program. In the study, a hyperbolic curve is used to describe both the stress-softening and the stress-hardening form of load deflection characteristics observed on light pavements. A method of determining the nonlinear elastic material properties for the base course and the subgrade using the falling weight deflectometer or the Dynaflect was developed. From the data collected with the pavement dynamic cone penetrometer, it appears that the stiffness of the granular base course depends, not surprisingly, on the degree of compaction of the material. The model adopted for accumulated permanent deformation due to repetitive loading and reloading follows a hyperbolic-shaped load deflection curve with a linear unloading path. Thick pavements, which are usually the stress-hardening type, appear to be more resistant to rutting. The new approach is shown to be accurate in predicting the development of rut depth with repeated loads applied by a variety of different vehicles. A computer program is written to incorporate the complete analysis method.

As a result of increasing industrial and agricultural activities, heavier trucks and higher traffic volumes have accentuated the problem of load rating and zoning of various farm-to-market roads that have light pavement structures. In evaluating overweight vehicle permit applications, the present practice in Texas is to determine the gross allowable loads on the light pavement structure by performing Texas triaxial tests on cored samples (C. McDowell, Wheel Load Stress Computations Related to Texas Highway Department Triaxial Method of Flexible Pavement Design, unpublished report of the Texas Highway Department). A more efficient, nondestructive testing method of determining damage to pavements by overweight vehicles is needed.

The new approach is a computerized procedure that uses results obtained from the Dynaflect or the falling weight deflectometer (FWD) to determine the number of passes of a specified load that will cause a critical level of rut depth in a light pavement structure. Conversely, the maximum allowable load on a light pavement structure can be determined using rut depth as a criterion for unacceptability. Rut depths are caused by accumulating pavement deformation under repeated load applications. Each time a load passes, the pavement fails to rebound as much as it was deflected under load. Establishing the difference between the loading and the unloading path is critical to making a reliable prediction of rut depth. Some of the advantages of the new approach are

1. Nondestructive testing (NDT) will reduce the time and the manpower currently required to deter-